Proceedings of the 8th International Symposium on Mathematical Morphology,
Rio de Janeiro, Brazil, Oct. 10–13, 2007, MCT/INPE, v. 1, p. 363–374.
http://urlib.net/dpi.inpe.br/ismm@80/2007/03.05.12.30

Morphological texture gradients: Definition and application to colour and texture watershed segmentation

Jesús Angulo

Centre de Morphologie Mathématique (CMM), Ecole des Mines de Paris, Fontainebleau, France
jesus.angulo@ensmp.fr

Abstract This paper deals with a morphological approach to calculate texture gradients and it is shown how to use them for image segmentation according to the texture; and more generally, for joint colour/texture segmentation (i.e., structural segmentation). The starting point is a decomposition of the colour image into two components: the object layer and the texture layer. A multi-scale local analysis from the texture layer is built using morphological operators (openings/closings or levelings) to define the gradients of texture. The proposed texture gradient is then combined with the colour gradient to produce mixed segmentations by watershed.

Keywords: granulometry, leveling, colour/texture decomposition, colour gradient, texture gradient, watershed transform.

1. Introduction

The classical paradigm of morphological segmentation is the watershed transformation with imposed markers [14], which is one of the most powerful segmentation techniques. Watershed-based hierarchical approaches allow addressing fields where markers cannot be easily defined (e.g., natural images, video-surveillance, etc.). Two main hierarchical techniques can be distinguished: 1) non-parametric waterfalls algorithm [4], which eliminates the contours completely surrounded by stronger contours; and 2) hierarchies based on extinction values [12, 20], which allow to select the minima used in the watershed according to different morphological criteria (in particular, the volume, which combines the size and the contrast of the regions, defines a good criterion to evaluate the visual relevance of regions). These algorithms are built on a scalar gradient. A colour gradient must be calculated to apply the watershed on a colour image. According to our previous works [2], we propose to compute a complete colour gradient in a luminance/saturation/hue representation, which is relatively robust towards illumination condition variations. More precisely, if

Proceedings of the 8th International Symposium on Mathematical Morphology,
Rio de Janeiro, Brazil, Oct. 10–13, 2007, MCT/INPE, v. 1, p. 363–374.
http://urlib.net/dpi.inpe.br/ismm@80/2007/03.05.12.30

$\mathbf{f}(x) = (f_L(x), f_S(x), f_H(x))$ denotes a colour image in the LSH representation, its colour gradient is given by:

$$\varrho_{col}(\mathbf{f})(x) = (1 - f_S(x)) \times \varrho(f_L)(x) + f_S(x) \times \varrho^{\circ}(f_H)(x) + \varrho(f_S)(x),$$

where $\varrho(g)(x)$ is the morphological gradient of a scalar function $g(x)$ (in this case, the luminance $f_L(x)$ and the saturation $f_S(x)$) and $\varrho^{\circ}(a)(x)$ is the circular centered gradient of an angular function $a(x)$ (in this case, the hue component $f_H(x)$).

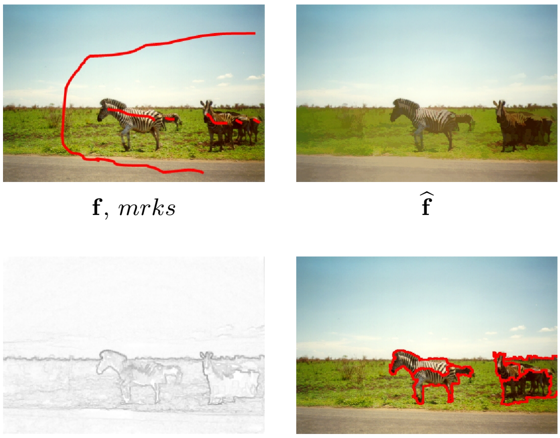

$\mathbf{f}, mrks$ $\widehat{\mathbf{f}}$

$\varrho_{col}(\widehat{\mathbf{f}})$ $Wshed(\varrho_{col}, mrks)$

Figure 1. Example of colour segmentation by markers-based watershed.

In the traditional way to segment an image by watershed transformation, the colour image is previously filtered by means of a connected operator, typically a leveling [13], $\lambda(m, f)$ (f is the reference image and $m(f)$ is the marker image, which is a rough simplification of the reference image), which simplifies textures and eliminates small details, but preserving the contours of remaining objects. For colour images, a marginal leveling can be applied for each component R, G, B or a total colour leveling can be calculated [1]. In any case, the leveling needs an image marker which determines the structures to be preserved, i.e.,

$$\widehat{\mathbf{f}} = \lambda(ASF_{nB}(\mathbf{f}), \mathbf{f}),$$

where ASF_{nB} is an alternate sequential filter of size n and B is an isotropic structuring element (other filters such as the Gaussian filters can be used to build the marker). Then, the watershed is calculated on the colour gradient of $\widehat{\mathbf{f}}$. The example of Figure 1 illustrates the segmentation with a marker for each object of interest (each zebra and an additional marker for the

Proceedings of the 8th International Symposium on Mathematical Morphology,
Rio de Janeiro, Brazil, Oct. 10–13, 2007, MCT/INPE, v. 1, p. 363–374.
http://urlib.net/dpi.inpe.br/ismm@80/2007/03.05.12.30

background). As we can observe, the colour information does not make possible to extract correctly the object contours.

Indeed, the texture is in certain images a very discriminating information for object separation. However, to introduce texture into the segmentation is not so simple as for the colour: texture is a regional notion which is difficult to quantify. In [6], Hill et al. proposed a method to build a texture gradient starting from a wavelet transformation, which is then used with the watershed to segment grey-level images. The combined use of colour and texture is the topic of a certain number of recent works. Ma and Manjunath [8] introduced the interest of Gabor filters for texture image segmentation. Vanhamel et al. introduced in [21] a marginal approach to apply Gabor filters to each component of a colour image and thus to construct a colour/texture feature space for segmentation. In a similar way, Hoang et al. [7] used Gabor filters to measure colour/texture and the segmentation is obtained by k-means. The works by Malik et al. [10] are also based on banks of Gaussian filters to calculate a texture gradient which is then combined with luminance and colour gradients in a supervised learning framework. Sofou et al. [18] introduced a joint intensity/texture segmentation by a PDE-based watershed, where texture is measured by a demodulation filter bank. This last work starts from an image decomposition according to the model $f = u + v$ by Y. Meyer [15], where u is the "cartoon component" (homogeneous zones of the objects) and v is the "texture oscillation". This model was initially studied within the framework of a variational approach by Vese and Osher [22]. More recent works, for example Patwardhan and Sapiro [16] and Aujol et al. [3], explore fast variational algorithms for the calculation of the images u and v. Sofou et al. proposed to obtain the texture component as the residue of a leveling, i.e., $v = f - u = f - \lambda(m, f)$ (the marker m is a Gaussian filter of f).

In this paper, we focus on a similar framework to that of Sofou et al. [18], but less expensive in computational terms. Our starting point is also a colour image decomposition of $\mathbf{f}$ into two components:

$$\mathbf{f} \triangleq \widehat{\mathbf{f}} \uplus f_{tex},$$

where $\widehat{\mathbf{f}}$ is the *object layer* and f_{tex} is the *texture layer*. The texture layer is obtained as the residue of the components of luminance, i.e., $f_{tex} = f_L - \widehat{f_L}$, because the texture variations are mainly associated to the luminance.

2. Granulometries and morphological multi-scale analysis

A granulometry is the study of the size distribution of the objects of an image [11, 17]. Formally, for the discrete case, a granulometry is a family of openings $\Gamma = (\gamma_n)_{n\geq 0}$ that depends on a positive parameter n (which expresses a size factor) such as: 1) $\gamma_0(f) = f$; 2) $f \leq g \Rightarrow \gamma_n(f) \leq \gamma_n(g), \forall n \geq$

Proceedings of the 8th International Symposium on Mathematical Morphology,
Rio de Janeiro, Brazil, Oct. 10–13, 2007, MCT/INPE, v. 1, p. 363–374.
http://urlib.net/dpi.inpe.br/ismm@80/2007/03.05.12.30

0, $\forall f, g$; 3) $\gamma_n(f) \leq f, \forall n \geq 0$, $\forall f$; 4) and γ_n verifies the semi-group absorption law; i.e., $\forall n, m \geq 0$, $\gamma_n\gamma_m = \gamma_m\gamma_n = \gamma_{\max(n,m)}$. Moreover, a granulometry by closings (or anti-granulometry) can be defined as a family of increasing closings $\Phi = (\varphi_n)_{n\geq 0}$. In practice, the most useful granulometry and anti-granulometry are those associated to morphological openings/closings: $\gamma_n(f) = \delta_{nB}(\varepsilon_{nB}(f))$ and $\varphi_n(f) = \varepsilon_{nB}(\delta_{nB}(f))$ respectively, where B is a structuring element of unit size (typically a disc or a segment of straight line) and $n = 1, 2, \cdots$. The greedy algorithms for granulometries involve consequently openings (closings) of increasing size, and thus they are relatively expensive. However, optimised fast algorithms for granulometry computation have been developed by Vincent [23].

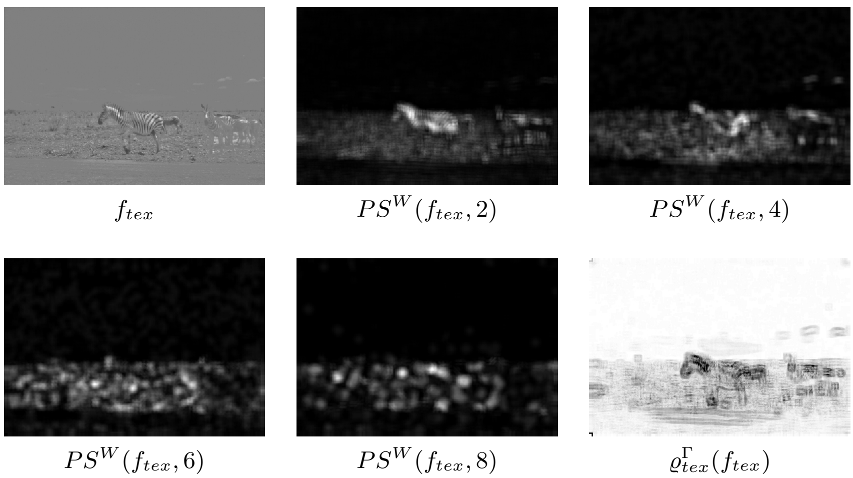

Figure 2. Texture layer, local granulometry (window $W_x = 10 \times 10$) by isotropic openings, morphological texture gradient.

The granulometric analysis of an image f with respect to Γ consists in evaluating each opening of size n with a measurement: $\mathcal{M}(\gamma_n(f))$ (where $\mathcal{M}$ is the integral of scalar function values). The granulometric curve, or pattern spectrum [9], of f with respect to Γ and Φ, $PS_{\Gamma,\Phi}(f, n)$ or $PS(f, n)$, is defined by the following normalised mapping:

$$PS(f, n) = \frac{1}{\mathcal{M}(f)} \begin{cases} \mathcal{M}(\gamma_n(f)) - \mathcal{M}(\gamma_{n+1}(f)), & for\ \ n \geq 0, \\ \mathcal{M}(\varphi_{|n|}(f)) - \mathcal{M}(\varphi_{|n|-1}(f)), & for\ \ n \leq -1. \end{cases}$$

The value of pattern spectrum $PS(f, n)$ for each size n corresponds to a measurement of bright structures of size n (similarly, the dark structures are obtained by closings). The pattern spectrum $PS(f, n)$ is a probability density function (i.e., a histogram): a peak or mode in PS at a given scale n indicates the presence of many image structures of this scale or size.

Proceedings of the 8th International Symposium on Mathematical Morphology,
Rio de Janeiro, Brazil, Oct. 10–13, 2007, MCT/INPE, v. 1, p. 363–374.
http://urlib.net/dpi.inpe.br/ismm@80/2007/03.05.12.30

Granulometric size distributions can be used as descriptors for texture classification. However, the texture descriptor $PS(f,n)$ is global to the image f, and if f contains more than one texture, the classification should be carried out at pixel level. This is the concept behind the granulometric local analysis [5], which consists in calculating a local pattern spectrum, or more precisely a pattern spectrum in a window $W_x = size_h \times size_v$ ($size_h$ is the horizontal size in pixels and $size_v$ the vertical one) centered at pixel x. The local pattern spectrum $PS^{W_x}(f,n)$, or simply $PS^W(f,n)$, is obtained by computing the function $PS(f_{W_x}, n)$ for each pixel x, where f_{W_x} is the restriction of the image f to the window W_x. This method is very expensive from a computational viewpoint. A faster approach to obtain $PS^W(f,n)$ is based on the computation of only one series of openings/closings and then, for each pixel x, to calculate locally the integral in W_x, i.e., $\mathcal{M}^{W_x}(g) = \sum_{y\in W_x} g(y)$. As result of this computation, a granulometric curve is obtained for each pixel. This local texture descriptor can be used to classify the various zones of texture in an image [5].

In our case, this local granulometric analysis must be done on the texture layer f_{tex} and the series of images which code this analysis is denoted by $\{t_k^{\Gamma\Phi}(x)\}_{k\in K} = \mathbf{t}^{\Gamma\Phi}(x)$, where

$$t_k^{\Gamma\Phi}(x) = PS^{W_x}(f_{tex}, k).$$

The function $t_k^{\Gamma\Phi}(x)$ is named the image of local energy of size k ($k \geq 0$ for the bright structures and $k \leq -1$ for the dark structures). In Figure 2 the texture layer for the image of zebras is shown, as well as the images of local energy associated to the local granulometry by isotropic openings (window $W_x = 10 \times 10$ and $K = \{-16, -14, \cdots, -2, 2, 4, \cdots, 16\}$). It is observed that the structures of f_{tex} have high values of local energy for their corresponding sizes. In the example, only four images $t_k^{\Gamma}(x)$ are shown (bright structures); a dual analysis $t_k^{\Phi}(x)$ provides the local energies for the different scales of dark structures. The choice of the size of the window depends on the "texture scales". However, its influence is limited: for all the examples of natural images presented in this study the choice $W_x = 10\times 10$ showed to be appropriate. In Figure 3 another example of colour/texture decomposition is given, including also two images of local energy. Obviously we can use other non isotropic structuring elements B in order to describe, for example, orientated textures.

In mathematical morphology, we can build other multi-scale analysis using other operators different from openings/closings. Let $ASF_n(f) = \varphi_n\gamma_n \cdots\ \varphi_2\gamma_2\ \varphi_1\gamma_1(f)$ be the alternate sequential filter of size n (we can define another family of filters by reversing the order of the opening/closing). The family $\Xi = (ASF_n)_{n\geq 0}$ verifies the semi-group law of absorption and consequently, it allows to define multi-scale simplification (or selection, by considering the residues) of the structures of f_{tex}. In addition, if each scale is associated to a leveling, the new family of transformations, $\Lambda = (\lambda_n)_{n\geq 0}$

Proceedings of the 8th International Symposium on Mathematical Morphology,
Rio de Janeiro, Brazil, Oct. 10–13, 2007, MCT/INPE, v. 1, p. 363–374.
http://urlib.net/dpi.inpe.br/ismm@80/2007/03.05.12.30

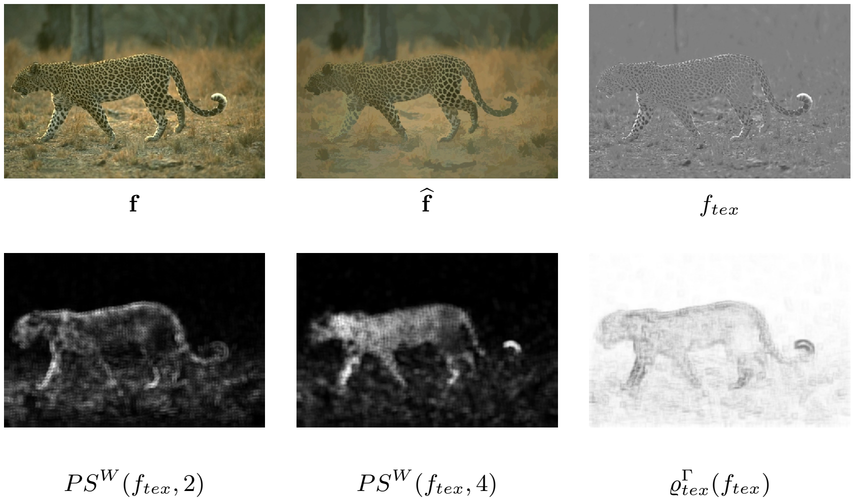

Figure 3. Colour/texture decomposition, two images of local energy, morphological texture gradient.

such that $\lambda_n(f) = \lambda(ASF_n(f), f)$, provides a decomposition of the reconstructed objects according to each scale n. It should be noted that using the levelings, both bright/dark objects of size n appear in the same image.

This leveling-based quantitative analysis of the objects associated to each size n makes it possible to define a pseudo-granulometric curve, named Λ-pattern spectrum, which is defined as follows:

$$\Lambda PS(f, n) = \mathcal{M}(\lambda_n(f)) - \mathcal{M}(\lambda_{n-1}(f)),$$

for $n \geq 0$. As for the granulometry, a local version of $\Lambda PS(f, n)$ is defined by computing the measure in a window W centered in each pixel. The associated series of images of local energy, i.e.,

$$t_k^{\Lambda}(x) = \Lambda PS^{W_x}(f_{tex}, k),$$

gives an alternative multi-scale representation (typically $k \in K = \{2, 4, \cdots, 16\}$). It must be remarked that for $t_k^{\Gamma\Phi}$ and t_k^{Λ} the maximal size k is limited by the size of leveling used to build $\widehat{\mathbf{f}}$, e.g., the maximal size of structures in f_{tex}. Other morphological multi-scale decompositions could be used in order to define other texture descriptors: operators associated with dynamics, area, volume, etc. [19, 20].

3. Morphological gradients of texture

We consider now the alternatives to calculate a gradient, associated to the multi-scale analysis, which allows determining the contours for the zones of

Proceedings of the 8th International Symposium on Mathematical Morphology,
Rio de Janeiro, Brazil, Oct. 10–13, 2007, MCT/INPE, v. 1, p. 363–374.
http://urlib.net/dpi.inpe.br/ismm@80/2007/03.05.12.30

different textures.

In each point x, the morphological gradient $\varrho(x)$ of unit size $B(x)$ of an image g can be written in terms of increments, i.e., $\varrho(g)(x) = \delta_B(g)(x) - \varepsilon_B(g)(x) = \vee[g(x) - g(y), y \in B(x)]$. Using this formulation, it is possible to use an Euclidean distance to define a gradient of morphological type for the series of images of local energy, i.e.,

$$\varrho_{tex}(f_{tex})(x) = \vee_y[d_E(\mathbf{t}(x), \mathbf{t}(y)), y \in B(x)],$$

where $d_E(\mathbf{t}(x), \mathbf{t}(y)) = \sqrt{\sum_{k \in K}(t_k(x) - t_k(y))^2}$ is the Euclidean distance between the two pixels x and y for all the images of local energy.

Besides this vectorial gradient, it is also possible to define another kind of gradient, by combining the gradients of each scalar image of energy. Various tests showed that the gradient by supremum, i.e.,

$$\varrho_{tex}(f_{tex})(x) = \bigvee_{k \in K}[\varrho(t_k(x))],$$

is as useful for the segmentation as the vectorial gradient defined by Euclidean distance, and easier to compute. Figure 2 gives also the morphological gradient $\varrho^{\Gamma}_{tex}(f_{tex})$ calculated according to the sup of scalar gradients. For the example of Figure 3, the gradient has been computed using the vectorial formulation.

Figure 4. Examples of markers-based watershed segmentation with texture gradients and structural gradients (colour+texture), i.e., $Wshed(\varrho, mrks)$.

These texture gradients, derived from the images of local energy $\{t^{\Gamma\Phi}_k(x)\}$ and $\{t^{\Lambda}_k(x)\}$, respectively $\varrho^{\Gamma\Phi}_{tex}(x)$ and $\varrho^{\Lambda}_{tex}(x)$, can be used with the watershed to segment the image into regions according to the texture. See the

Proceedings of the 8th International Symposium on Mathematical Morphology,
Rio de Janeiro, Brazil, Oct. 10–13, 2007, MCT/INPE, v. 1, p. 363–374.
http://urlib.net/dpi.inpe.br/ismm@80/2007/03.05.12.30

two corresponding results in Figure 4, to be compared with the colour segmentation of Figure 1. As we can observe, both texture gradients segment correctly the region of each zebra (which are certainly defined by their texture), such as we wanted. However, we can also note that the contours of the obtained regions are not very precise. Indeed, the segmentation according to a texture gradient gives rough regions.

4. Structural gradient for watershed-based joint colour/texture segmentation

The approach to produce a structural segmentation consists in constructing a joint gradient of colour and texture. Once both a colour gradient and a texture gradient are available, it seems obvious that we can combine them to obtain the called structural gradient. Among the different alternatives for the combination of gradients, we retained two of them which appear particularly simple to implement and sufficiently flexible to evaluate the influence of a gradient with respect to the other. In fact, it deals, on the one hand, with the sum of the colour gradient and a weighted texture gradient (to control the influence of the second one); and on the other hand, with a barycentric linear combination of both gradients. In mathematical terms, we have:

$$\begin{aligned}
\varrho_{str}^{I-\alpha}(\mathbf{f})(x) &= \varrho_{col}(\widehat{\mathbf{f}})(x) + \alpha\varrho_{tex}(f_{tex})(x), \\
\varrho_{str}^{II-\alpha}(\mathbf{f})(x) &= (1-\alpha)\varrho_{col}(\widehat{\mathbf{f}})(x) + \alpha\varrho_{tex}(f_{tex})(x),
\end{aligned}$$

where $0 \leq \alpha \leq 1$. For both cases, $\varrho_{col}(x)$ and $\varrho_{tex}(x)$ correspond to the definitions previously introduced in the paper. It is obvious that both structural gradients are essentially equivalent; moreover, permitting $\alpha > 1$, identical linear combinations could be obtained. However, as remarked above, the aim of $\varrho_{str}^{I-\alpha}(\mathbf{f})(x)$ is to incorporate the information of texture gradient as a secondary term with respect to the colour, whereas the barycentric formulation $\varrho_{str}^{II-\alpha}(\mathbf{f})(x)$ defines a trade-off between texture/colour gradients. In addition, the inherent normalisation of equation $\varrho_{str}^{II-\alpha}(\mathbf{f})(x)$ preserves the dynamic range of the final gradient image, which could be necessary for watershed computation. We could also consider that the weighting values are not constant for all the image points; or in other words, to define for instance $\varrho_{str}^{II-\alpha}(\mathbf{f})(x) = (1-\alpha(x))\varrho_{col}(\widehat{\mathbf{f}})(x) + \alpha(x)\varrho_{tex}(f_{tex})(x)$, where $\alpha(x)$ is the local weighting function. The appropriate computation of $\alpha(x)$ is out of the scope of this paper.

Figure 4 shows a comparison of segmentation by watershed on the image of zebras according to various structural gradients. We observe that for the texture analysis based on openings/closings as well as for that based on levelings, the balanced structural gradient, i.e., $\varrho_{str-\Gamma\Phi}^{I-\alpha=1}(\mathbf{f})$ and $\varrho_{str-\Lambda}^{I-\alpha=1}(\mathbf{f})$ respectively, improves the segmentations compared to the colour gradient

Proceedings of the 8th International Symposium on Mathematical Morphology,
Rio de Janeiro, Brazil, Oct. 10–13, 2007, MCT/INPE, v. 1, p. 363–374.
http://urlib.net/dpi.inpe.br/ismm@80/2007/03.05.12.30

$\varrho_{col}(\widehat{\mathbf{f}})$. In addition, for this example, we observe also that the best result corresponds to $\varrho^{II-\alpha=0.8}_{str-\Gamma\Phi}(\mathbf{f})$; (texture here is more appropriate than the colour). Moreover, the fact of combining the texture gradient with the colour gradient leads to more precise contours.

To complement the results of our study, we tested the structural gradients on a series of natural colour images and we evaluated the colour segmentation vs. the structural segmentation by watershed. Figure 5 shows four representative images: Examples 1–3 correspond to the segmentation by marker-based watershed (a marker for the object of interest and a marker for the background) and Examples 4–6 correspond to the volume-based segmentation into 50 regions. For each image the segmentation according to the colour gradient and the structural segmentation according to a balanced colour+texture for the two families of texture descriptors that we studied in the paper ($\varrho^{I-\alpha=1}_{str-\Gamma\Phi}$ and $\varrho^{I-\alpha=1}_{str-\Lambda}$) are given. Due to the fact that it is difficult to know *a priori* for an image if it is the colour or the texture which constitutes the most relevant information for the segmentation, we think that the most judicious choice is a balanced combination of this type.

We note that for the example of the butterfly, the structural segmentation is always more coherent than that of the colour. With $\varrho^{I-\alpha=1}_{str-\Gamma\Phi}$, only a part of the wings is obtained (which have same colour-texture) and with $\varrho^{I-\alpha=1}_{str-\Lambda}$ the two colour-textures of the wings are taken into account, producing a perfect segmentation. A similar analysis can be made for the segmentation of the image 2 (a marker following the people and another for the background). In this case, the "texture" corresponds to the head and clothes details of the people. The image of the tiger is a good counterexample which shows that if the texture between the object of interest and the background is very similar, the fact of using a structural gradient will probably introduce a biased segmentation (an intermediate result is obtained using the barycentric linear combination with a greater weight for the colour gradient than for the texture gradient).

For the segmentation of complex images into 50 regions which contain well contrasted coloured objects as well as large areas with or without texture. We see that the structural gradient makes it possible to improve the well-known problem of the volume-based watershed which over-segments the large and homogeneous areas (e.g., sky in Image 4). In addition, certain objects of small size are better segmented with the structural gradients. The contribution of texture allows finding the contours of certain texture zones which are not determined by the colour, as can be observed on Images 5 and 6.

Finally, it is difficult to affirm generally, and without more exhaustive and systematic tests in a large database, if the partitions for $\varrho^{I-\alpha=1}_{str-\Gamma\Phi}$ are more relevant than those for $\varrho^{I-\alpha=1}_{str-\Lambda}$. We observe from the examples that in random textures (e.g., tiger or bear fur, natural textures of Image 6) the segmentation associated to an openning/closing granulometry, $\varrho^{I-\alpha=1}_{str-\Gamma\Phi}$, is more satisfactory. In other examples, where the notion of texture is more

Proceedings of the 8th International Symposium on Mathematical Morphology,
Rio de Janeiro, Brazil, Oct. 10–13, 2007, MCT/INPE, v. 1, p. 363–374.
http://urlib.net/dpi.inpe.br/ismm@80/2007/03.05.12.30

related to certain significant structures (e.g., the image of the butterfly), the gradient $\varrho^{I-\alpha=1}_{str-\Lambda}$ from the pseudo-granulometry of connected filters seems to be more appropriate.

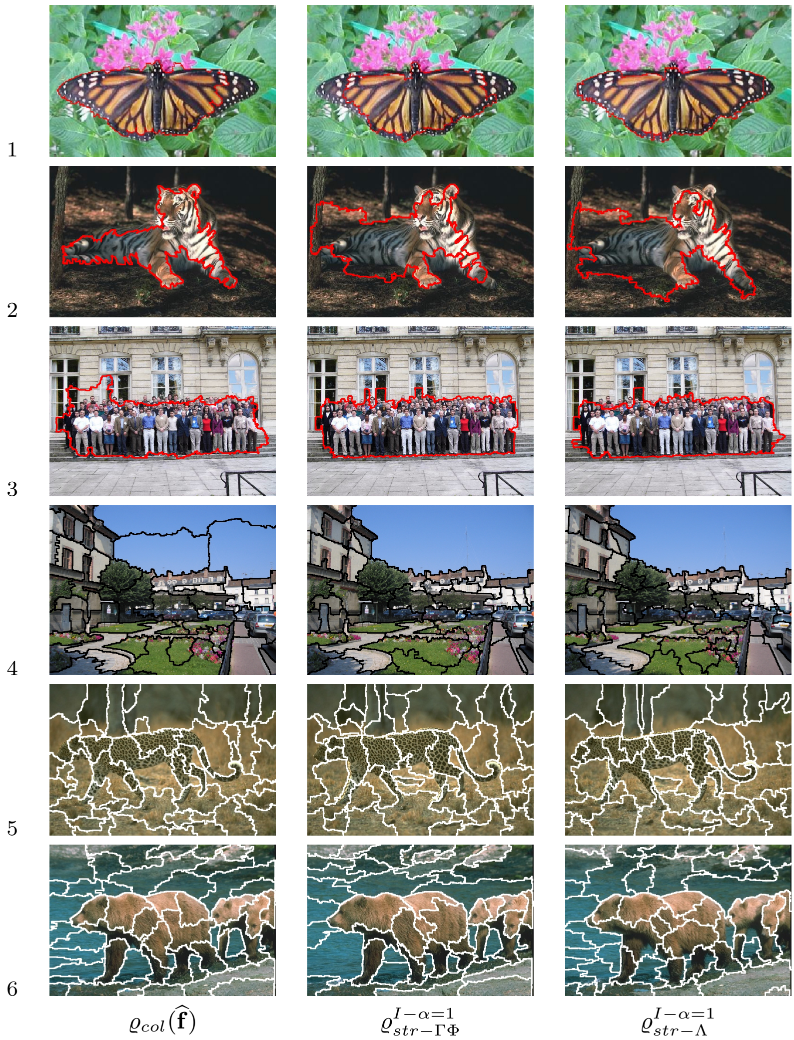

Figure 5. Watershed-based colour segmentation versus structural segmentation. Examples 1–3, markers for objects; Examples 4–6, selection of 50 volumic regions.

Proceedings of the 8th International Symposium on Mathematical Morphology,
Rio de Janeiro, Brazil, Oct. 10–13, 2007, MCT/INPE, v. 1, p. 363–374.
http://urlib.net/dpi.inpe.br/ismm@80/2007/03.05.12.30

5. Conclusions and perspectives

This paper presented a morphological approach to calculate texture gradients and it showed how to use them for image segmentation according to the texture; and more generally, for joint colour/texture segmentation (i.e., structural segmentation). We illustrated that these gradients are directly usable for morphological segmentation by watershed and that the partitions obtained with structural gradients are, in most of cases, more relevant than those obtained only with colour gradients. In particular, we showed that the areas of texture are better determined and that the over-segmentation of large and homogeneous zones is reduced.

At present, we are interested in the definition of colour-texture decompositions, without limiting the texture layer to the luminance information. Our purpose is to evaluate the interest of residues of colour openings/levelings (for instance, colour operators defined by means of total orderings in the luminance/ saturation/ hue representation). In addition, we are working on an automatic and local combination of the gradients of colour and texture such that this coupling of information should be adapted to the local image characteristics (i.e., computation of function $\alpha(x)$).

References

[1] J. Angulo, *Morphological colour image simplification by saturation-controlled regional levellings*, Pattern Recognition **20** (2006), no. 8, 1207–1223.

[2] J. Angulo and J. Serra, *Modelling and Segmentation of Colour Images in Polar Representations*, Image Vision and Computing **25** (2007), no. 4, 475–495.

[3] J.-F. Aujol, G. Gilboa, T. Chan, and S. Osher, *Structure-Texture Image Decomposition - Modeling, Algorithms, and Parameter Selection*, International Journal of Computer Vision **67** (2006), no. 1, 111–136.

[4] S. Beucher, *Watershed, hierarchical segmentation and waterfall algorithm*, ISMM'94 (1994), Mathematical Morphology and its Applications to Image and Signal Processing, pp. 69–76.

[5] E. R. Dougherty, J. T. Newell, and J. B. Peltz, *Morphological texture-based maximum likelihood pixel classification based on local granulometric moments*, Pattern Recognition **25** (1992), 1181–1198.

[6] P. R. Hill, C.N. Canagarajah, and D. R. Bull, *Image segmentation using a texture gradient based watershed transform*, IEEE Transactions on Image Processing **12** (2003), no. 12, 1618–1633.

[7] M. A. Hoang, J.-M. Geusebroek, and A. W. M. Smeulders, *Color texture measurement and segmentation*, Signal Processing **85** (2005), 265–275.

[8] W. Y. Ma and B. S. Manjunath, *EdgeFlow: A technique for boundary detection and segmentation*, IEEE Transactions on Image Processing **9** (2000), no. 8, 1375–1388.

[9] P. Maragos, *Pattern Spectrum and Multiscale Shape Representation*, IEEE Trans. on Pattern Analysis and Machine Intelligence **11** (1989), 701–716.

[10] D. R. Martin, C. C. Fowlkes, and J. Malik, *Learning to Detect Natural Image Boundaries Using Local Brightness, Color, and Texture Cues.*, IEEE Trans. on Pattern Analysis and Machine Intelligence **26** (2004), 1–20.

Proceedings of the 8th International Symposium on Mathematical Morphology,
Rio de Janeiro, Brazil, Oct. 10–13, 2007, MCT/INPE, v. 1, p. 363–374.
http://urlib.net/dpi.inpe.br/ismm@80/2007/03.05.12.30

[11] G. Matheron, *Ensembles aléatoires et géométrie intégrale. Tome II*, Ecole des Mines de Paris, Les Cahiers du Centre de Morphologie Mathématique, Fascicule 6, 1972.

[12] F. Meyer, *An Overview of Morphological Segmentation*, International Journal of Pattern Recognition and Artificial Intelligence **15** (2001), no. 7, 1089–1118.

[13] ______, *Levelings, Image Simplification Filters for Segmentation*, Journal of Mathematical Imaging and Vision **20** (2004), 59–72.

[14] F. Meyer and S. Beucher, *Morphological segmentation*, Journal of Visual Communication and Image Representation **1** (1990), no. 1, 21–45.

[15] Y. Meyer, *Oscillating Patterns in Image Processing and Nonlinear Evolution Equations*, AMS, University Lecture Series Vol. 22, 2002.

[16] K. A. Patwardhan and G. Sapiro, *Automatic Image Decomposition*, ICIP'04 (2004), IEEE International Conference on Image Processing, Vol. I, pp. 645–648.

[17] J. Serra, *Image analysis and mathematical morphology, Vol. I*, Academic, London, 1982.

[18] A. Sofou, G. Evangelopoulos, and P. Maragos, *Coupled geometric and texture PDE-based segmentation*, ICIP'05 (2005), IEEE International Conference on Image Processing, Vol. II, pp. 650–653.

[19] C. Vachier, *Morphological Scale-Space Analysis and Feature Extraction*, ICIP'01 (2001), IEEE International Conference on Image Processing, Vol. III, pp. 676–679.

[20] C. Vachier and F. Meyer, *Extinction value: a new measurement of persistence*, (1995), IEEE Workshop on Nonlinear Signal and Image Processing, pp. 254–257.

[21] I. Vanhamel, A. Katartzis, and H. Sahli, *Hierarchical segmentation via a diffusion scheme in color/texture feature space*, ICIP'03 (2003), IEEE International Conference on Image Processing, Vol. I, pp. 969–972.

[22] L. Vese and S. Osher, *Modeling textures with total variation minimization and oscillating patterns in image processing*, J. Sci. Comp. **19** (2003), 553–572.

[23] L. Vincent, *Local grayscale granulometries based on opening trees*, ISMM'96 (1996), Mathematical Morphology and its Applications to Image and Signal Processing, pp. 273–280.